A novel approach for measuring the void fraction in stratified air-water systems utilizing an 8-blade capacitance-based sensor, sinogram, and a deep neural network

Abdulilah Mohammad Mayet[1], Mohammad Hossein Shahsavari[2],
Seyed Mehdi Alizadeh[3], Robert Hanus[4*] [iD], Muneer Parayangat[1], Ramkumar M. Raja[1],
Mohammed Abdul Muqeet[1], Mohammed Arafath Salman[1], Piotr Kubiszyn[4]

[1] Electrical Engineering Department, King Khalid University, Abha 61411, Saudi Arabia
[2] Independent Researcher, Muscat 123, Oman
[3] Department of Petroleum Engineering, College of Engineering, Australian University, West Mishref, Safat 13015, Kuwait
[4] Faculty of Electrical and Computer Engineering, Rzeszów University of Technology, Powstańców Warszawy 12, 35-959, Rzeszów, Poland
* Corresponding author's e-mail: rohan@prz.edu.pl

ABSTRACT

Measuring void fraction (VF) in a pipeline is crucial for ensuring operational efficiency, safety, and environmental responsibility in various engineering applications. There are several methods commonly used to measure VF in multiphase flow systems. Capacitance sensors are a dependable and practical option for measuring VF, providing benefits such as versatility, sensitivity, cost-effectiveness, and ease of use. In this study, simulations were performed to produce different VF levels of an air-water stratified two-phase flow, ranging across 31 distinct VF values from completely full to entirely empty. Moreover, an 8-blade concave capacitive sensor was designed and utilized for VF measurements. In order to use the power of the finite element method (FEM), COMSOL multiphysics was employed to produce the desired void fractions and measure the capacitance value of each pair of electrodes. The capacitance values of these electrode pairs were measured, resulting in the creation of sinograms corresponding to different VF. These sinograms were utilized as inputs for a deep neural network (DNN) developed in Python, specifically a Multilayer Perceptron model, to estimate VFs. Furthermore, to enhance user understanding, sinograms were employed to reconstruct fluid images using the back-projection method. The results demonstrated an accuracy of 0.002, a significant improvement over previous methodologies in VF measurement.

Keyword: two-phase flow, void fraction, stratified flow pattern, capacitance-based sensors, concave sensor, flow measurement, tomography.

INTRODUCTION

Horizontal two-phase flow plays a vital role in various industrial processes and engineering systems such as oil and gas industry, power generation, chemical processing, HVAC systems, and nuclear power plants. Understanding and accurately predicting the behavior of two-phase flow in horizontal pipes is essential for optimizing performance, ensuring safety, and achieving cost-effective operation in a wide range of applications. Measuring void fraction is essential for optimizing processes, ensuring safety, maintaining product quality, mitigating environmental risks, managing resources efficiently, and advancing scientific knowledge [1–3]. Accurate void fraction measurements are indispensable across a wide range of industries and applications, contributing to improved performance, reliability, and sustainability [1–3].

Various methods are employed for measuring void fraction in pipelines. Capacitance sensors detect void fraction by measuring the changes in the dielectric properties of the fluid mixture. Gamma-ray attenuation involves passing gamma rays through the flow and measuring the attenuation caused by the presence of fluid [4–5]. Ultrasonic techniques utilize sound waves to measure the time taken for waves to travel through the mixture, indicating changes in void fraction [6–7]. Pressure drop measurements correlate changes in pressure drop across a section of the flow channel with void fraction variations and so many other methods [8].

Void fraction refers to the ratio of the volume of void (such as gas) to the total volume within a two-phase flow system. Figure 1 illustrates the image of a cross-section view of a pipeline and the geometrical formula of the void fraction is shown, where A_{liquid} and A_{gas} represents the area filled with the liquid phase and the area filled with the gas. It is not far from imagination to realize that measuring void fraction using a capacitance-based method has stood out as an important topic for scientists because it offers a number of advantages. For example, the method doesn't disrupt ongoing flow patterns. Moreover, it can provide more information on the flow characteristics, such as flow pattern classification, scale detection, and even tomography. At the heart of ensuring capacitive sensors operate with precision and accuracy lies in the meticulous design of electrodes. It's essential to configure these electrodes in alignment with the critical properties of the fluid undergoing measurement. This process may entail various configurations, including concave, ring, or helical

Figure 1. Void fraction in a stratified two-phase flow and geometric formula

structures, each optimized to efficiently capture specific dynamic properties of the flowing fluid within the pipeline [9–13]. Prior research in this domain has unveiled three primary flow patterns within pipelines – stratified, annular, and homogeneous – each possessing distinct characteristics requiring tailored approaches to achieve successful measurement. Abulwafa's study delves into capacitance designs aimed at discerning volume fractions in two-phase pipelines. Through experimental comparisons, the research evaluates various structures, particularly focusing on slug (SL) and stratified (ST) flow patterns. The findings suggest that while the double helix capacitance stands out as the most practical linear sensor, a four-concave-plate structure might offer superior sensitivity and construction simplicity under specific flow pattern conditions [14]. In [15] Ahmed outlines the design methodology for capacitance sensors tailored to void-fraction measurement in two-phase flow systems. Through theoretical and experimental analyses focusing on concave and ring sensor configurations, it was found that ring-type sensors exhibit higher sensitivity to void-fraction signals compared to concave types with similar spatial resolution. Moreover, the theoretical model's predictions for ring-type sensors demonstrate better alignment with experimental data, supported by comprehensive analyses including mean value, time trace, power spectral density (PSD), and probability density function (PDF) of void-fraction signals. In [16] Reis and his colleagues delve into the complexities of measuring volumetric concentrations in two-phase flows within industrial pipelines and equipment. By exploring the effectiveness of capacitive probes, particularly focusing on various geometric configurations of electrodes like helical, double ring, and concave structures, the study sheds light on their unique characteristics and challenges. Through meticulous experimentation and comparison, the findings highlight the double-ring configuration as the optimal choice for accurately measuring volumetric concentrations in two-phase air-water flows. Extensive research led by Hammer and his colleagues focused on advancing a helical electrode capacitance sensor, which represented a significant breakthrough in accurately measuring water fraction and undissolved gas in crude oils, presenting a notable enhancement in precision compared to conventional non-intrusive sensors [17]. Wang and his colleagues introduced an innovative capacitive array sensor
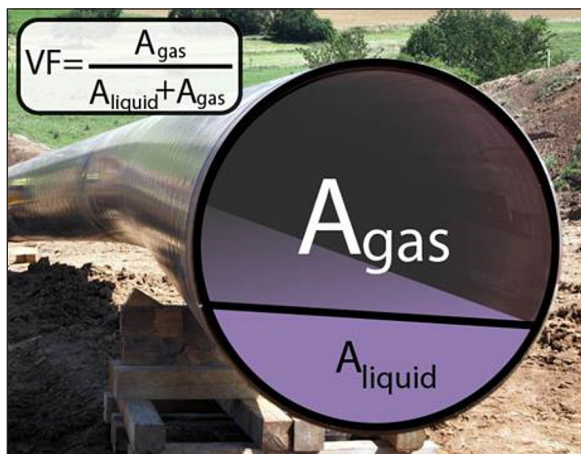
that combines flow pattern recognition with void fraction measurement, thereby improving accuracy through a validation method verified on a specialized air-water two-phase flow experimental platform [18]. Chen and his colleagues introduced an innovative multi-wire capacitance probe technique aimed at accurately measuring void fraction in stratified gas-liquid flow, as a result, they made notable enhancements in precision and thorough analysis of flow parameters [19]. In [20] Jaworek's research introduces a radio-frequency resonance sensor equipped with a variable capacitance mechanism for precise gas-liquid volume ratio measurements. By employing semi-cylindrical electrodes positioned externally on a dielectric pipeline, the sensor detects variations in capacitance induced by changes in the gas and liquid percentages. The resulting frequency deviations in the oscillator, tuned to 80 MHz, serve as a reliable indicator of the two-phase flow composition within the pipe, offering insights into volume ratios with significant accuracy. Aluisio and his colleagues outlined and demonstrated the design and testing of an electrical capacitance sensor aimed at monitoring two-phase water-oil flow. Their study encompasses an analysis of different sensor geometries [21]. The paper by Zhuoqun [22] investigates the correlation between alterations in flow patterns and flow rates in two-phase oil-gas flows by employing dual ECT sensors, a linear projection algorithm, and a convolutional neural network (CNN) algorithm for prediction. ElasticNet regression is utilized to address overfitting concerns. Kendoush and Sarkis (1995) explored void fraction measurements using the capacitance method, assessing five capacitor configurations: parallel, strip-type plates, ring-type plates, unidirectional, and double-helix. Their research simulated void fractions using various systems like nonflow air-paraffin wax, air-glass, air-wood, and air-Freon 113, aiming to minimize relative statistical errors through careful consideration of electrode spacing [23]. In [24] Krupa introduces a novel method for void fraction measurement in small-channel two-phase flows using capacitance sensors. The approach involves utilizing a high-frequency oscillator connected to a resonant circuit, allowing direct determination of void fraction from a calibration curve. By numerically analyzing changes in electrode capacitance corresponding to different void fractions, Krupa demonstrates the efficacy of this method in accurately characterizing two-phase flow dynamics.

In [25] a direct-imaging sensor utilizing multiple capacitance measurements, utilized by Vendruscolo et al., they introduced, a prototype sensor constructed and evaluated across diverse scenarios, demonstrating strong concordance with a reference sensor. Lusheng conducted thorough research wherein they established an equivalent circuit model for a concave capacitance sensor designed for stratified oil-water flow. Their study involved the simultaneous detection of real and simulationary response signals, as well as experimental exploration of the influences of flow pattern on excitation frequency [26]. Kim et al. undertook the development of a calibration method for capacitance measurements of void fraction in refrigerant flow, they figured a non-linear relationship influenced by flow patterns and it was validated experimentally [27]. Mayet and his co-workers worked on different problems of using capacitance-based sensors such as dependency on temperature and pressure [28].

In [28], the focus is on homogeneous flow patterns, utilizing a combined capacitance-based sensor with concave and ring sensors, and employing COMSOL Multiphysics simulations to train an artificial neural network (ANN), achieving a mean absolute error (MAE) of 4.868. In contrast, this study examines stratified flow patterns using an 8-blade concave capacitive sensor. It generates 31 distinct void fractions through COMSOL Multiphysics and uses the resulting capacitance values to create sinograms, which serve as inputs for a DNN model, achieving an accuracy of 0.002. Additionally, this work enhances interpretability through sinogram-based fluid image reconstruction. While Mayet's approach targets homogeneous flow with integrated sensor types and ANN-based predictions, this study emphasizes accuracy and interpretability in stratified flow, highlighting the potential of advanced computational techniques in void fraction measurement.

Fouladina et al. studied using capacitance-based sensors dependency on changes in liquid phase in a two-phase flow regime [29].

In our previous study [30], the challenge of accurately determining phase fractions in two-phase flows prevalent in power plants and petrochemical industries was addressed. Through a comprehensive approach that included finite element simulations, experimental validations using concave electrode shapes, and the development of an ANN model, void fractions were

successfully predicted with an error of less than 2% for various liquid-gas combinations, providing a precise metering solution for annular two-phase flows with different liquids. The volume fraction of each phase in two-phase flows is addressed in a previous study [31], focusing on stratified two-phase flow scenarios commonly encountered in petrochemical industries. Several experiments were conducted on vertical concave, horizontal concave, and double-ring sensors to validate simulation results obtained via COMSOL Multiphysics software. The simulation data, confirmed by experimental data, highlighted the higher overall sensitivity of concave sensors compared to double-ring sensors, with horizontal concave sensors exhibiting greater sensitivity at higher void fractions and vertical ones at lower void fractions. Moreover in a previous work [32], a new electrode configuration was explored for void fraction measurement in two-phase flows using capacitance-based sensors. The proposed 'skewed' sensor, characterized by its unique geometric shape, underwent evaluation and enhancement through simulations conducted with COMSOL Multiphysics software. These simulations covered various flow patterns, and assessed the influences of geometric properties on sensor sensitivity, yielding an optimized configuration. Moreover, sensitivity distribution analysis across different void fractions and comparison with alternative sensors demonstrated the proposed sensor's notably higher overall sensitivity, crucial in the petroleum industry for precise multiphase flow metering. Various advanced techniques have been explored for accurate flow measurement, including the development of novel sensor designs and methods for better flow rate estimation. For example, AL Jarrah introduced a technique using single and double coil sensors to enhance flow rate measurement accuracy [33], while another study utilized magnetic coupling for flow sensing in pure water environments [34]. These approaches align with this study's focus on integrating advanced sensor technology for improved measurement precision.

The primary objective of this paper is to measure void fraction with a high degree of accuracy. Various techniques are utilized for this purpose in pipelines. Capacitance sensors determine void fraction by detecting changes in the dielectric properties of the fluid mixture. Gamma-ray attenuation involves passing gamma rays through the flow and measuring the attenuation caused by the presence of fluid. Ultrasonic techniques use sound waves to measure the time it takes for the waves to travel through the mixture, indicating changes in void fraction. Pressure drop measurements correlate changes in pressure drop across a section of the flow channel with variations in void fraction. Each of these methods provides unique insights and advantages for accurately assessing void fraction in two-phase flow systems.

This work introduces a novel method for measuring void fractions with exceptional accuracy, utilizing a fluid sinogram and a neural network. The reason behind selecting an 8-blade concave instead of a sensor with a larger number of blades is that because of the bigger cross section it would offer a higher signal-to-noise ratio and lower error related to the velocity of flow which, makes it suitable for use in high-speed fluid environments. Additionally, a tomographic image has been developed to enhance user insights. In this investigation, simulations were conducted with the aim of generating diverse void fractions within an air-water stratified two-phase flow, encompassing a range from completely full (0) to entirely vacant (1). An 8-blade concave capacitive sensor is used. Leveraging the FEM, COMSOL Multiphysics facilitated the generation of desired void fractions and measurement of capacitance values across different electrode pairs. The resulting capacitance values were used to construct sinograms corresponding to varying void fractions. These sinograms served as inputs for an Artificial Neural Network model, specifically a multilayer perceptron (MLP) implemented in Python, to estimate the void fractions. Additionally, sinograms were utilized in fluid image reconstruction via the back-projection method to enhance user comprehension. Figure 2 shows the methodological flowchart of the paper making the overall procedure of the current paper much more clear. This study introduces a novel approach that combines sinogram-based analysis with a DNN for accurate void fraction measurement. Unlike traditional methods, our approach uses sinograms derived from an 8-blade concave capacitance sensor as inputs for a neural network, achieving improved accuracy and interpretability, with an error margin as low as 0.002.

In this paper, the structure is outlined as follows: First, the benchmark and simulation parameters and features are discussed in the Simulation Properties section to ensure reproducibility. Next, in the Sensor Geometry and Analyses section, the
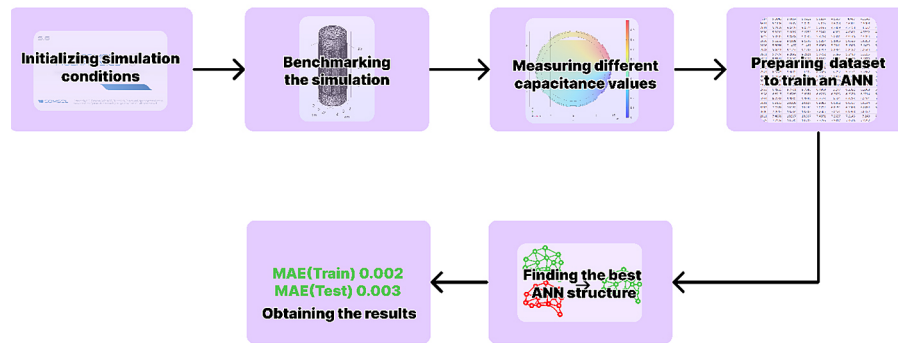
Figure 2. Methodological flowchart of the paper

physical dimensions and geometry of the proposed concave sensor are covered, different combinations of capacitance values are examined, and sinograms for each void fraction are generated. In the ANN and Back Projection section, the process of obtaining void fractions and creating tomographic images from the sinograms is detailed. Furthermore, in the Results and Discussion section, the model's accuracy is presented and compared to other works in terms of lower mean absolute error, and the implications of the findings are discussed, along with suggestions for future research.

SIMULATION PROPERTIES

The aim of this study was to quantify the void fraction within a two-phase flow comprising air and water, emphasizing stratified flow patterns. In stratified gas-liquid flow, distinct separation between gas and liquid phases occurs as they traverse confined spaces such as pipelines. The establishment of a stratified flow regime is influenced by factors such as fluid characteristics, pipe diameter, flow velocities, and surface tension. To evaluate the reliability of the COMSOL Multiphysics application, a previous investigation [31] conducted a thorough assessment of its functionality and precision. The aforementioned research conducted both experimental and simulation analyses to compare various tests applied to a stratified air-liquid two-phase flow. Upon comparing the simulation outcomes with the experimental data, the reliability and credibility of COMSOL Multiphysics performance and accuracy were established. The experimental setup of the mentioned paper is shown in Figure 3. The GPS-3135C LCR meter used in experiments can accurately measure capacitance values ranging from 0.00001 pF to 9999.99 mF, with a frequency range of 50 Hz to 100 kHz and a test signal resolution of 10 mV. This ensures precise capacitance readings, which are crucial for our analysis. The PLA pipe used in the experiments had a relative permittivity of 3.3.
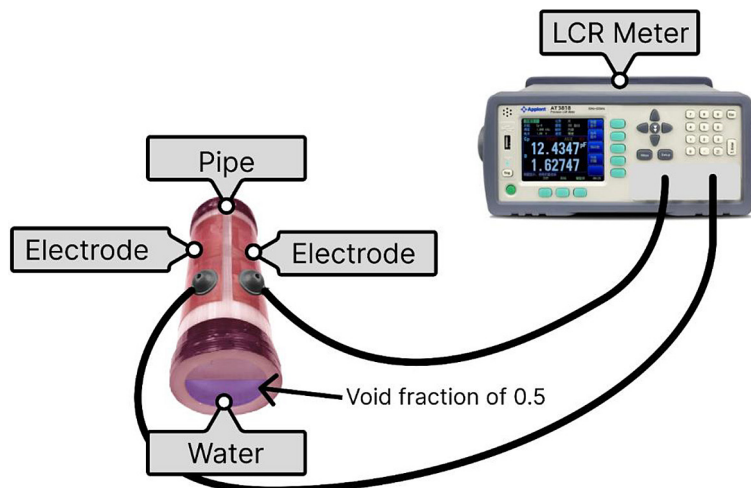
Figure 3. Experimental setup from the previous work as described in reference [31]

COMSOL Multiphysics stands out as a highly regarded software solution extensively employed across diverse sectors. Leveraging the FEM, it constructs tailor-made simulations for a wide array of industrial applications, encompassing mechanical, and electronic domains among others. The potent electric fields enveloping the capacitor plates make it necessary to form a gaseous zone within the simulation, setting the necessary stage for our analyses. Notably, as the gap widens between the electrodes, the electric field weakens, demonstrating an inverse correlation with the cube of the gap's size. A static examination is undertaken, given the constancy of factors shaping the electrical field across time. Employing the finite element approach, renowned for its efficacy in delivering precise outcomes, the COMSOL simulation software adeptly executes simulations, as previously emphasized. COMSOL offers a range of meshing options, and for this particular simulation, the resulting structure is configured and resolved using the finite element technique within the COMSOL simulation environment. To enhance the result fidelity, the mesh granularity has been fine-tuned. This technique involves deploying a network of elements for meticulous computations and assessments. The utilization of a finer mesh necessitates shrinking the size of individual elements, as delineated in Table 1, defining the dimensions of distinct components. The mesh model is created using a physics-controlled mesh sequence, which automatically adjusts mesh refinement and coarsening based on the underlying physical characteristics, such as specific geometric features and boundary conditions. The computational operation was performed on a computing device outfitted with an Intel 11th generation i3 processor and 8 gigabytes of random-access memory (RAM). Table 2 shows the specific parameters that are considered during the simulation.

Table 1. Characteristic of the meshed model

Feature	Value
The maximum size of element	0.7 cm
The minimum size of element	0.03 cm
The maximum element growth rate	1.35
Curvature factor	0.3
The resolution of narrow areas	0.85
Number of vertex elements	92
Number of edge elements	4645
Number of boundary elements	79935
Number of elements	638170
Free meshing time	7 sec
Minimum element quality	0.07466

Table 2. The parameter settings for simulations

Feature	Value
Space dimension	3D
Physics interface	Electrostatics
Type of study	Stationary
Studied parameter	Maxwell capacitance

Figure 4. Geometric properties of electrodes and pipeline (a), (b), and the meshed model of the presented sensor (c)

SENSOR GEOMETRY AND ANALYSES

To utilize the 8-blade concave sensor, the benchmarked software application is employed. The schematic representation of the simulated 8-blade concave electrode, including its dimensions and composition, is depicted in Figure 4a and Figure 4b. Throughout the simulation process, precision is set to a finer level, leading to the subdivision of the geometry into 638,170 domain elements. The meshed model is visually depicted in Figure 4c. Displayed in Figure 4, the sensor with an 8-blade concave design consists of eight distinct electrodes colored in pink, brown, lime, dark blue, purple, maroon, orange, and dark purple. They possess a length of 12 cm with a 5 mm spacing between them. The main purpose of this paper is to measure void fraction and construct a tomography image of flow to give the user better insights. Figure 5 shows the desired goal of this paper therefore, In order to perform a forward projection and create the sinogram the capacitance values for various combinations are measured.

The primary objective of this study is to assess the void fraction from sinogram and generate a tomographic representation of fluid flow, aimed at enhancing user understanding. The main goal of the tomography is to see how the material inside the pipe is distributed. Tomography is well-known as a good technique in medicine and basically, it has two main stages: forward projection and back projection. There are several methods for projecting such as using gamma ray attenuation or x-ray attenuation or sound-based methods like sonar methods even the measurements using electrical resistance and so many other methods. So all the mentioned methods are used in order to create the sinogram image, for reconstructing images there are several mathematical algorithms like ART, SART, BP, and FBP. To create the tomography image a technique called backprojection is used. It is well-known for its computational simplicity which will result in real-time capability. Therefore, capacitance measurements are conducted across different configurations to perform forward projections and the creation of a sinogram. In other words, the sinogram is the measured capacitance values for different pairs of electrodes. Figure 6 shows the sinogram of 0.5. As shown in Figure 6 the capacitance values of the specific combination of electrodes are measured and the result is shown in Figure 6 where the yellow color shows a higher
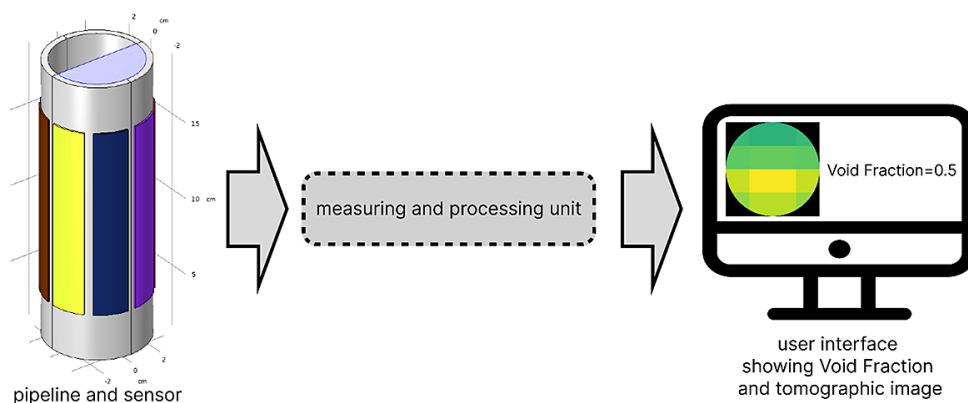
Figure 5. Representation of the main goal of this paper
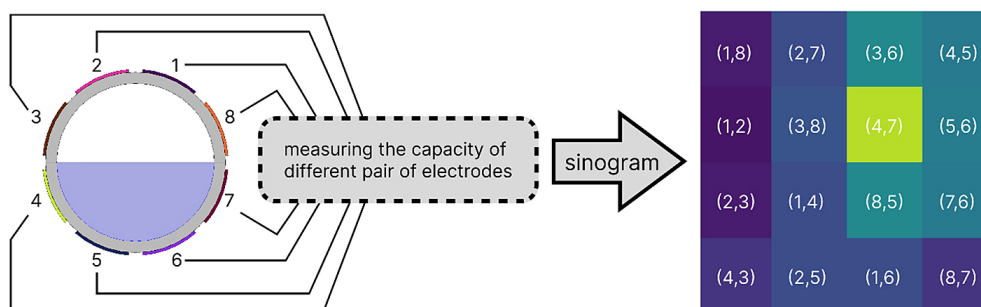
Figure 6. Diagram of creation of sinogram

value and the purple color stands for lower values. In the matrix's third column and second row, electrodes numbered 4 and 7 are highlighted. It's evident that due to water's high relative permittivity of 81 compared to air's relative permittivity of 1, this specific pixel exhibits the highest recorded value. Similarly, considering the pixel situated in the first column and second row, associated with electrodes 1 and 2, it's notable that these electrodes register the lowest value, presumably due to their considerable distance from the water surface.

ARTIFICIAL NEURAL NETWORK AND BACK PROJECTION

The main novelty of this paper is to calculate the void fraction with much higher accuracy compared to similar works using the new approach that involves ANN and sinogram of the pipe. Within the expansive landscape of Artificial Intelligence (AI), its applications span a multitude of sectors including retail, finance, transportation, education, fault diagnosis, energy consumption management, and notably, healthcare. Among these, healthcare emerges as a focal point for AI's transformative capabilities. Particularly noteworthy is its role in revolutionizing medical imaging analysis [35]. By leveraging AI algorithms, radiologists can achieve unprecedented levels of accuracy in detecting various pathologies from complex medical imagery, thus paving the way for more efficient and precise diagnoses and treatments. The utilization of AI transcends singular dimensions; it encompasses a broad and multifaceted spectrum. ANNs and DNNs wield a plethora of applications. These are highly precise mathematical methodologies employing computational nodes known as neurons, organized into single or multiple layers [36]. DNNs and ANNs excel particularly in tasks such as prediction and classification, each exhibiting distinct forms tailored to specific applications. DNNs aim to mimic the information processing mechanisms of the human brain, mirroring ANNs. DNNs comprise multiple concealed layers nestled between input and output layers [37]. Typically, a network is constructed using datasets earmarked for training and testing purposes. The training dataset comprises a specific set of sample inputs utilized to train the neural network, while the test dataset contains new information unseen by the network. This dataset is employed to scrutinize and authenticate the network's predictive prowess. For the deep learning calculations, TensorFlow library with the Keras API due to its flexibility and ease of use was utilized in building neural networks. Additionally, NumPy was used for data manipulation, and Matplotlib assisted in visualizing the training process and results. Discovering the optimal configuration for a DNN demands thorough experimentation with various parameters. This entails fine-tuning the number of processing epochs, adjusting network layers, and selecting appropriate activation functions. Following extensive testing, the most efficient network architecture is identified and proposed for the novel metering system. In the scope of this study, a DNN model is specifically tailored with 16 inputs, representing the value of each pixel of sinogram which is the capacitance values derived from different combinations of an 8-blade capacitive sensor. Using the COMSOL Multiphysics software, 496 simulations are conducted, manipulating void fractions in increments of 0.03 from 0 to 1. Out of these simulations, 347 cases (70%) are allocated for training the network, while the remaining 149 cases (30%) are reserved for testing purposes. The key characteristics of the generated datasets are shown in Table 3. In developing the ANN model, a thorough hyperparameter tuning process was carried out to determine the optimal architecture. This process involved experimenting with various configurations, including the number of layers, neurons, learning rates, activation functions, and epochs. Each parameter was adjusted iteratively, emphasizing its significance. The number of layers was crucial for balancing network complexity and computational efficiency. The number of neurons influenced the model's learning capacity and helped prevent overfitting. Different activation functions (such as sigmoid, ReLU, and tanh) were evaluated to find the most effective one for our specific problem. Various

Table 3. The key parameters of datasets used in developing the model

Parameter	Value
Number of samples	500
Source of data	COMSOL simulations
Type of data	Number
Range and scale	4.57–15.01
Preprocessing steps	Normalize between 0 and 1
Split ratios	0.7 for Train and 0.3 for Test
Measurement conditions	25 °C

epochs were tested to identify the optimal point for convergence and avoid overfitting. Learning rates were also varied, with higher rates allowing larger adjustments and lower rates providing finer tuning of model parameters like weights and biases. Through extensive testing, the architecture that exhibited the best performance metrics was chosen. The final model's structure is the result of this comprehensive tuning process, ensuring high quality and performance. The steps taken to achieve the optimal structure are illustrated in Figure 7. Following numerous evaluations with different network configurations, considering diverse numbers of layers and neurons, the most suitable structure is identified. The detailed specifications of this configuration are outlined in Table 4. Figure 8 shows the tomography of the pipe and different void fractions. Once trained, the model's weights and biases are fixed, significantly reducing the computational burden. It can be deployed on a Raspberry Pi 4 Model B, ARM Cortex-M series microcontrollers with optimizations, FPGA
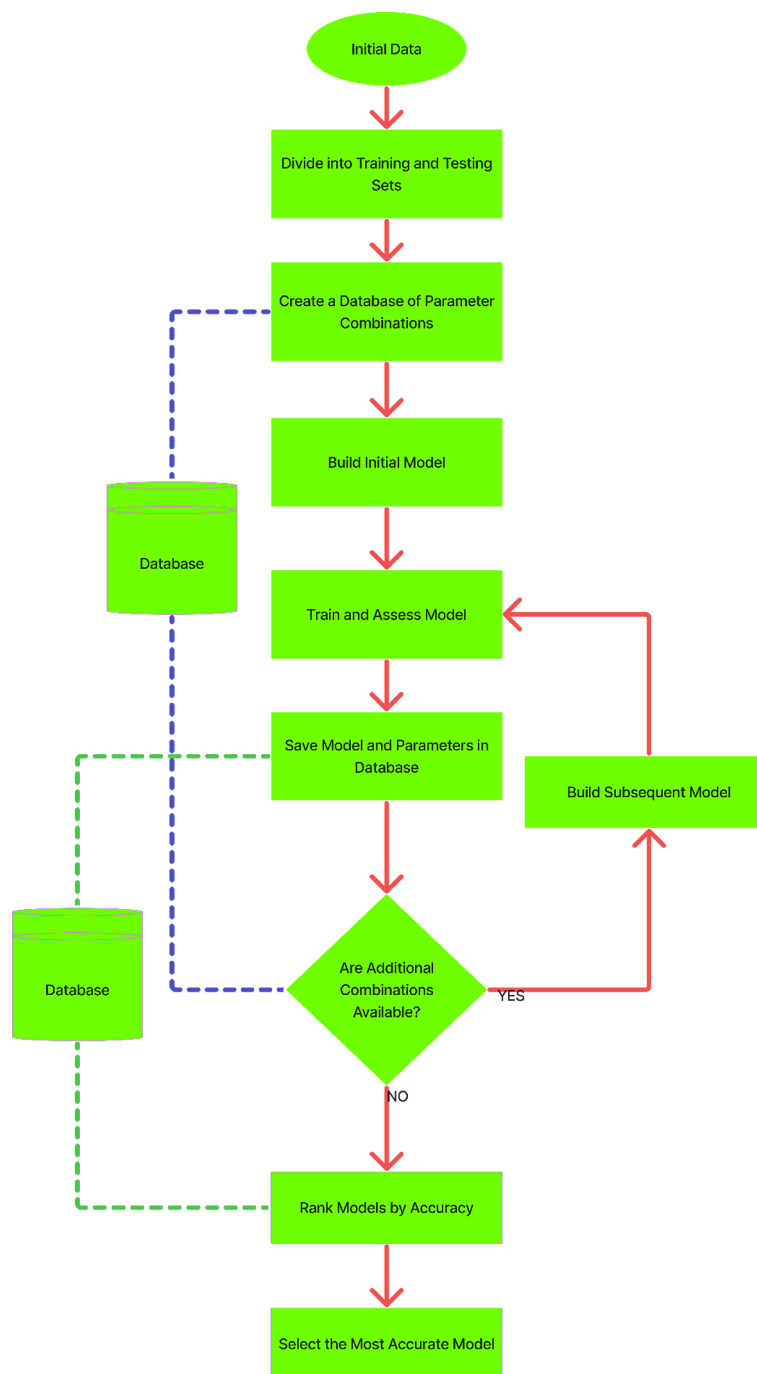
Figure 7. The process of obtaining the best ANN model

Table 4. Characteristics of proposed DNN

Parameter	Value
Learning rate	0.001
Neurons per layer	64
Type of network	Deep learning
Number of Inputs	16
Number of output layers	1
Number of epochs	500
Number of hidden layers	4
Hidden layers activation function	Rectified linear unit (ReLU)

boards like the Xilinx Zynq-7000 series for high performance, or cloud platforms such as AWS, Google Cloud, or Microsoft Azure. This flexibility ensures the model is practical for a wide range of devices and real-time applications.

RESULTS AND DISCUSSION

Measuring the void fraction is crucial for improving processes, ensuring safety, upholding product quality, reducing environmental hazards, using resources effectively, and enhancing scientific understanding. Precise void fraction measurements are vital in various industries and contexts, aiding in better performance, dependability, and eco-friendliness. In this paper, an 8-blade concave sensor is used to measure the capacitance values. The COMSOL Multiphysics has been used to utilize the FEM. 31 void fractions of stratified flow regimes are simulated for different combinations of electrodes. Using the measured values the date for creating the sinogram is produced. The primary novelty of this work is the significantly improved accuracy in measuring void fraction compared to previous studies. This was achieved through a novel approach that incorporates a fluid sinogram and a neural network. The sensor's 8-blade concave design provides greater sensitivity than sensors with more blades, making it ideal for high-speed fluid environments. Furthermore, the sensor's lower processing power requirements enhance its overall efficiency. Additionally, a tomographic image has been created to further improve user insights. the results show that this new method presents higher accuracy than previous approaches the mean absolute error of this model represented by Equation 1, is 0.002 for the training set and 0.003
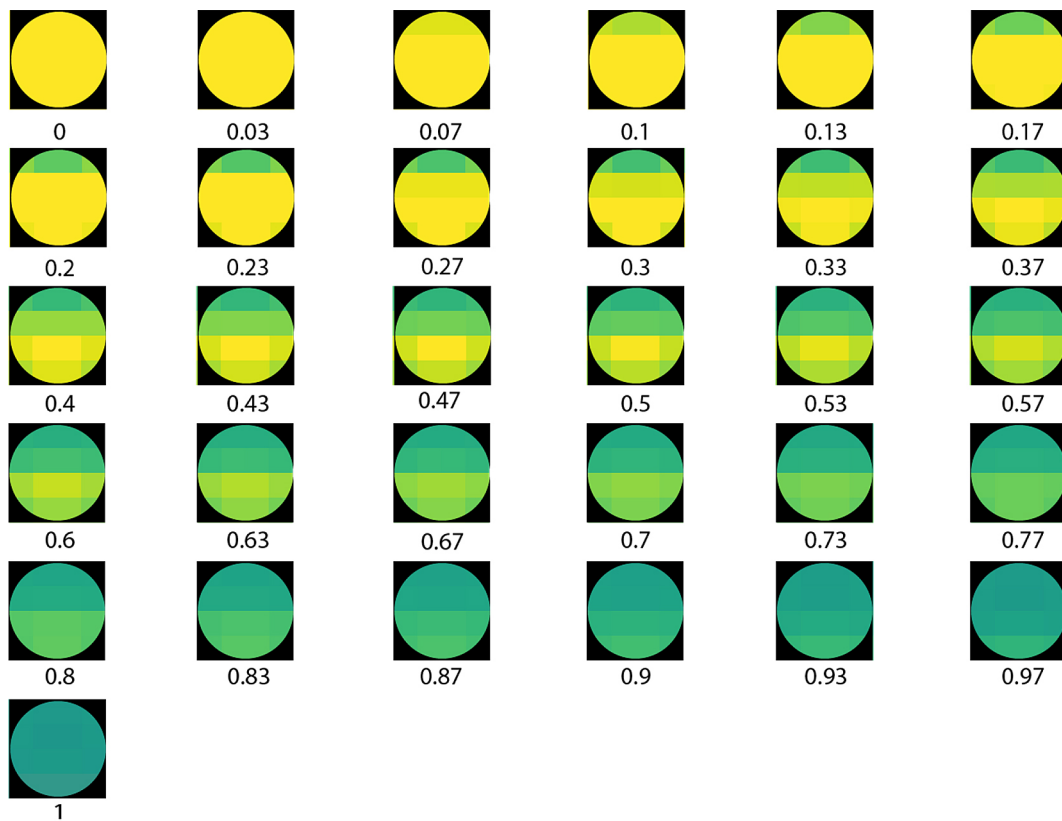
Figure 8. Reconstructed images of different void fractions

for the testing set. In the equation, N represents the data count, X(pred) denotes the predictions from the proposed MLP, and X(sim) corresponds to the simulated results from COMSOL. Another key parameter to demonstrate the correlation between the predicted data and the actual values is the Pearson correlation coefficient, as shown in Equation 2. In this formula x_i and y_i represent the predicted data points and actual data points, respectively, while $\overline{x}$ and $\overline{y}$ are the mean values of the predicted and actual data. The R^2 value, shown in Equation 3, indicates the strength and direction of the relationship between two variables. In this model, the R^2 value is 0.999 for the training dataset and 0.998 for the testing dataset, demonstrating a strong positive linear relationship between the variables.

$$MAE = \frac{1}{N} \sum_{i=1}^{N} |x_i(Sim) - x_i(Pred)| \qquad (1)$$

$$r = \frac{\sum (x_i - \overline{x})(y_i - \overline{y})}{\sqrt{\sum (x_i - \overline{x})^2 \sum (y_i - \overline{y})^2}} \qquad (2)$$

$$R^2 = r^2 \qquad (3)$$

Figure 9 shows the regression for training and testing data. As it is obvious the model is not facing any underfitting or overfitting. Moreover, the sinogram is used to reconstruct the flow pattern and gain some information about the distribution of material inside the pipe. This will give better insights into the flow pattern inside the pipe. Moreover, Table 5 presents a comparison between the results obtained in this study and those reported in other studies on void fraction measurements. The findings highlight notably improved accuracy compared to prior studies. Figure 10 illustrates the training and testing loss of the ANN model over 500 epochs. Initially, both training and testing losses decrease rapidly, indicating effective learning. Eventually, both losses stabilize and converge to near zero, demonstrating that the model has achieved optimal performance and minimal overfitting. The histogram of errors shown in Figure 11 reveals the distribution of prediction errors for

Table 5. Comparison of different studies measuring the void fraction

Reference	Approach	MAE (mean absolute error)	Feature selection	Output
[28]	MLP	0.048	-	Void fraction
[29]	MLP	0.049	-	Void fraction
[30]	MLP	0.012	-	Void fraction
[38]	RBF	0.04	Statistical features	Void fraction
[39]	RBF	0.05	Energy domain features	Void fraction
This study	Deep neural network	0.002	Sinogram matrix	Void fraction+tomographic image
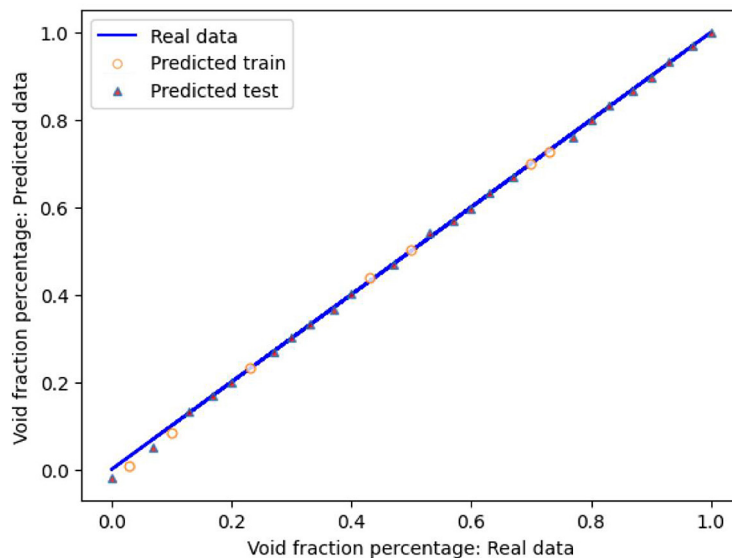
Figure 9. Regression of train, and test datasets with the prediction of them
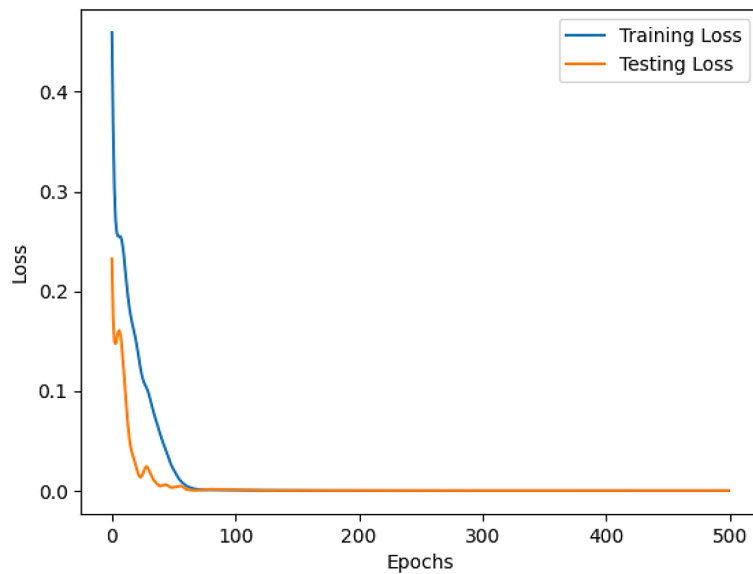
Figure 10. Loss function versus the number of epochs for training and testing datasets
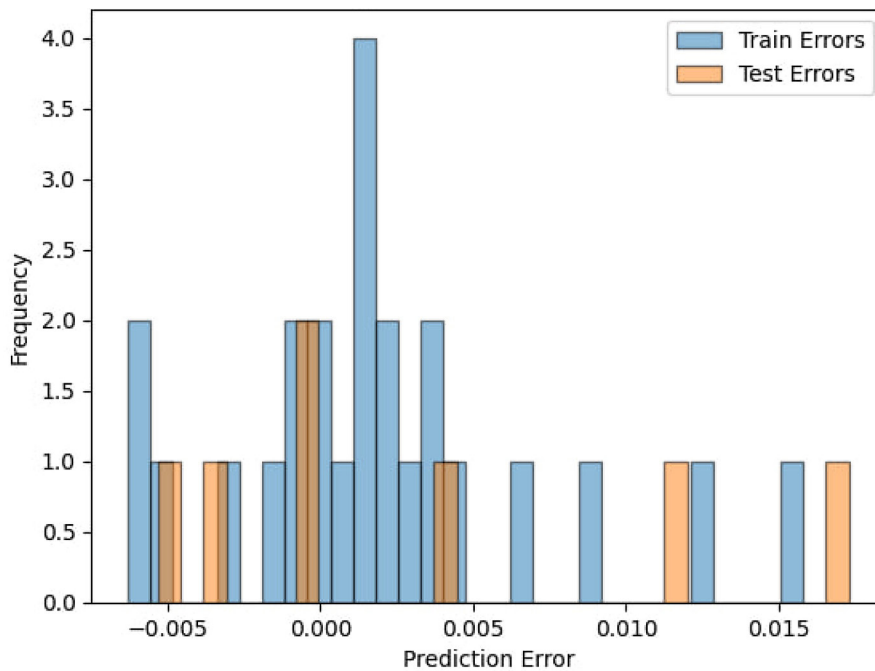
Figure 11. The histogram of errors for training and testing datasets

both training (blue) and testing (orange) datasets. Key observations include the centering of errors around zero, indicating no significant bias, and a relatively symmetrical distribution with most errors close to zero, suggesting high accuracy. The similarity in error distributions between training and testing datasets implies that the model generalizes well. These observations demonstrate that the model performs consistently and accurately on both datasets.

The primary innovation of this study was the achievement of significantly higher accuracy in void fraction measurements compared to previous methodologies. This advancement was attributed to the novel approach, which involved combining a fluid sinogram with a neural network. The deliberate choice of an 8-blade concave sensor, rather than a sensor with more blades, was made to leverage its larger cross-section, which provided a superior signal-to-noise ratio and effectively minimized errors associated

with flow velocity. This design was particularly advantageous in high-speed fluid environments and required less processing power, thus enhancing overall efficiency. Additionally, a tomographic image was developed to complement the measurements and improve user understanding. Overfitting is detected when a model is excessively fitted to a specific dataset, causing inadequate generalization to new data. To prevent overfitting in the model, several strategies were implemented. Firstly, the training and validation loss/accuracy were monitored. Overfitting is indicated when the training loss decreases while the validation loss begins to increase, or when training accuracy significantly exceeds validation accuracy. Additionally, learning curves were utilized to identify overfitting, as this can be observed if the training loss continues to decrease while the validation loss increases. Given that capacitance-based methods for measuring void fraction are significantly influenced by variations in relative permittivity due to changes in temperature and pressure, a novel approach that eliminates this dependency is needed. Utilizing the power of ANN presents a promising opportunity for future work. By employing ANNs, it is possible to develop a method that is independent of fluctuations in temperature and pressure, thereby improving the accuracy and reliability of void fraction measurements.

In practical applications, several potential sources of error could affect the accuracy of the measurements using the proposed method. These include: sensor calibration, electromagnetic interference, flow regime variability, pipe surface properties and noise in data acquisition. In light of the limitations observed, future research will focus on employing ANNs to develop a measurement method for void fraction that is independent of fluctuations in temperature and pressure. This approach aims to enhance both the accuracy and reliability of measurements. Furthermore, expanding the scope of this study to include various flow regimes, such as homogeneous or annular flows, will be explored. Investigations will also extend to different fluid types, including air-oil mixtures, and to fluids involving more than two phases. These advancements will help address the applicability of our findings to a broader range of flow patterns and fluid combinations, ultimately contributing to a more comprehensive understanding of void fraction measurement.

CONCLUSIONS

Measuring the void fraction within pipelines holds paramount importance in ensuring operational efficiency, safety, and environmental compliance across various engineering sectors. Numerous methodologies exist for gauging void fractions in multiphase flow systems. Capacitance sensors emerge as a dependable and practical option for void fraction assessment, offering versatility, sensitivity, cost efficiency, and user-friendliness as key advantages. To simulate diverse void fractions in an air-water stratified two-phase flow, simulations were executed spanning 31 void fractions ranging from complete occupancy (0) to complete emptiness (1). An 8-blade concave capacitive sensor was devised and deployed for void fraction measurements. Leveraging the FEM, COMSOL Multiphysics facilitated the generation of desired void fractions and the measurement of void fractions for each electrode pair. Capacitance values for these electrode pairs were gauged, yielding sinograms corresponding to various void fractions. These sinograms served as inputs for an ANN crafted in Python, specifically a Multilayer Perceptron model, to predict void fractions. Additionally, to enhance user comprehension, sinograms were utilized for fluid image reconstruction via the back-projection method. The outcomes showcased an accuracy level of 0.002, marking a noteworthy advancement over previous techniques in void fraction assessment. Future research can use ANNs to develop a void fraction measurement method independent of temperature and pressure fluctuations. Studies should also explore various flow regimes and fluid types, such as air-oil mixtures and multiphase fluids, to broaden the applicability of the findings.

REFERENCES

1. Gardenghi Á.R., Filho E.d.S., Chagas D.G., Scagnolatto G., Oliveira R.M., Tibiriçá C.B. Overview of void fraction measurement techniques, databases and correlations for two-phase flow in small diameter channels. *Fluids* 2020; 5(4): 216.

2. Sassi P., Pallarès J. & Stiriba Y. Visualization and measurement of two-phase flows in horizontal pipelines. Exp. Comput. Multiph. Flow 2020; 2: 41–51.

3. Khan U., Pao W., Sallih N. Numerical gas–liquid two-phase flow regime identification in a horizontal pipe using dynamic pressure data. *Applied Sciences* 2023; 13(2): 1225.

4. Sharifzadeh M., Khalafi H., Afarideh H., et al. Two-phase flow component fraction measurement using gamma-ray attenuation technique. Nuclear Science and Techniques 2017; 28: 88.

5. Roshani G.H., Nazemi E. A high performance gas–liquid two-phase flow meter based on gamma-ray :attenuation and scattering. Nuclear Science and Techniques 2017; 11: 169.

6. Fan J, Wang F. Review of ultrasonic measurement methods for two-phase flow. Review of Scientific Instruments 2021; 92: 091502.

7. Chang J.S., Ichikawa Y., Irons G.A., Morala E.C., Wan P.T. Void Fraction Measurement by an Ultrasonic Transmission Technique in Bubbly Gas-Liquid Two-Phase Flow. In: Delhaye, J.M., Cognet, G. (eds) Measuring Techniques in Gas-Liquid Two-Phase Flows. International Union of Theoretical and Applied Mechanics, Springer 1984.

8. Jia J., Babatunde A., Wang M. Void fraction measurement of gas-liquid two-phase flow from differential pressure. Flow Measurement and Instrumentation 2015; 41: 75–80.

9. Iliyasu A.M., Bagaudinovna D.K., Salama A.S., Roshani G.H., Hirot K. A methodology for analysis and prediction of volume fraction of two-phase flow using particle swarm optimization and :group method of data handling neural network. Mathematics 2023; 11(4): 916.

10. Al-lababidi S., Addali A., Yeung H., Mba D., Khan F. Gas void fraction measurement in two-phase gas/liquid slug flow using acoustic emission technology. J. Vib. Acoust. 2009; 131(6): 501–507.

11. Xie C.G., Stott A.L., Plaskowski A., Beck M.S. Design of capacitance electrodes for concentration measurement of two-phase flow. Meas. Sci. Technol. 1990; 1(1): 65–78.

12. Abdulkadir M., Hernandez-Perez V., Lowndes I.S., Azzopardi B.J., Brantson E.T. Detailed analysis of phase distributions in a vertical riser using wire mesh sensor (WMS). Experim. Thermal Fluid Sci. 2014; 59: 32–42.

13. Koyama S., Lee J., Yonemoto R. An investigation on void fraction of vapor-liquid two-phase flow for smooth and microfin tubes with R134a at adiabatic condition. Int. J. Multiphase Flow 2004; 30(3): 291–310.

14. Abouelwafa M.S., Kendall E.J. The use of capacitance sensors for phase percentage determination in multiphase pipelines. IEEE Trans. Instrum. Meas.

1980; 29: 24–27.

15. Ahmed H. Capacitance sensors for void-fraction measurements and flow-pattern identification in air–oil two-phase flow. IEEE Sens. J. 2006; 6: 1153–1163.

16. Dos Reis E., da Silva Cunha D. Experimental study on different configurations of capacitive sensors for measuring the volumetric concentration in two-phase flows. Flow Meas. Instrum. 2014; 37: 127–134.

17. Tollefsen J., Hammer E.A. Capacitance sensor design for reducing errors in phase concentration measurements. Flow Meas. Instrum. 1998; 9(1): 25–32.

18. Wang X., Chen Y., Wang B., Tang K., Hu H. Sectional void fraction measurement of gas-water two-phase flow by using a capacitive array sensor. Flow Meas. Instrum. 2020; 74: 101788.

19. He D., Chen S., Bai B. Void fraction measurement of stratified gas-liquid flow based on multi-wire capacitance probe. Experim. Thermal Fluid Sci. 2019; 102: 61–73.

20. Jaworek A., Krupa A. Gas/liquid ratio measurements by rf resonance capacitance sensor. Sens. Actuators A: Phys. 2004; 113: 133–139.

21. Wrasse A.D.N., Santos E.N.D., Silva M.J.D., Wu H., Tan C. Capacitive sensors for multiphase flow measurement: A review. IEEE Sensors J. 2022; 22(22): 21391–21409.

22. Xu Z., Wu F., Yang X., Li Y. Measurement of gas-oil two-phase flow patterns by using CNN algorithm based on dual ECT sensors with Venturi tube. Sensors 2020; 20(4): 1200.

23. Kendoush A.A., Sarkis Z.A. Improving the accuracy of the capacitance method for void fraction measurement. Exp. Therm. Fluid Sci. 1995; 11: 321–326.

24. Krupa A., Lackowski M., Jaworek A. Capacitance sensor for measuring void fraction in small channels. Measurement 2021; 175: 109046.

25. Wrasse A.D.N., Vendruscolo T.P., Santos E.N., Castaldo F.C., Morales R.E.M., da Silva M.J. Capacitive direct-imaging sensor for two-phase flow visualization. In: Proc. 2016 IEEE Sensors, 30 October–03 November 2016, 1–3.

26. Zhai L., Liu R., Zhang H., Jin N. Complex admittance detection of horizontal oil-water two-phase flows using a capacitance sensor. IEEE Sensors J. 2019; 19(17): 7489–7498.

27. [27] Kim M., Komeda K., Jeong J., Oinuma M., Sato T., Saito K. Optimizing calibration for a capacitance-based void fraction sensor with asymmetric electrodes under horizontal flow in a smoothed circular macro-tube. Sensors 2022; 22(9): 3511.

28. Mayet A.M., Ilyinichna G.E., Fouladinia F., Daoud M.S., Ijyas V.T., Shukla N.K., Habeeb M.S., Al-hashim H.H. An artificial neural network and a combined capacitive sensor for measuring the void

fraction independent of temperature and pressure changes for a two-phase homogeneous fluid. Flow Measurement and Instrumentation 2023; 93: 102406.

29. Chen T.C., Alizadeh S.M., Alanazi A.K., Grimaldo Guerrero J.W., Abo-Dief H.M., Eftekhari-Zadeh E., Fouladinia F. Using ANN and combined capacitive sensors to predict the void fraction for a two-phase homogeneous fluid independent of the liquid phase type. Processes 2023; 11(3): 940.

30. Veisi A., Shahsavari M.H., Roshani G.H., Eftekhari-Zadeh E., Nazemi E. Experimental study of void fraction measurement using a capacitance-based sensor and ANN in two-phase annular regimes for different fluids. Axioms 2023; 12(1): 66.

31. Shahsavari M.H., Veisi A., Roshani G.H., Eftekhari-Zadeh E., Nazemi E. An experimental and simulation study for comparison of the sensitivity of different non-destructive capacitive sensors in a stratified two-phase flow regime. Electronics 2023; 12(6): 1284.

32. Iliyasu A.M., Shahsavari M.H., Benselama A.S., Nazemi E., Salama A.S. An optimised and novel capacitance-based sensor design for measuring void fraction in gas–oil two-phase flow systems. Nondestructive Testing and Evaluation 2024: 1–17. https://doi.org/10.1080/10589759.2023.2301492

33. AL Jarrah A.M. A Novel simple technique for measuring the volumetric flow rate and direction of flow inside a pipe – the single and double coils sensors. Advances in Science and Technology Research Journal, 2022; 16(5): 290–298.

34. AL Jarrah A. M., Aljabarin N. Magnetic coupling of two coils due to flow of pure water inside them. Advances in Science and Technology Research Journal, 2022; 16(6): 203–212.

35. Jaber A.A., Khalid M.A. Artificial neural network based fault diagnosis of a pulley-belt rotating system, International Journal on Advanced Science. Engineering and Information Technology 2019; 9(2): 544–551.

36. Gallant A.R., White H. On learning the derivatives of an unknown mapping with multilayer feedforward networks. Neural Networks 1992; 5(1): 129–138.

37. Goodfellow I., Bengio Y., Courville A. Deep learning. Book in preparation for MIT Press. https://www.deeplearningbook.org

38. Jeshvaghani P.A., Saraee K.R.E., Feghhi S.A.H., Jafari A. Using statistical features and a neural network to predict gas volume fractions independent of flow regime changes. Flow Measurement and Instrumentation 2023; 93: 102430.

39. Roshani G.H., Nazemi E., Shama F., et al. Designing a simple radiometric system to predict void fraction percentage independent of flow pattern using radial basis function. Metrology and Measurement Systems 2018; 25(2): 347–358.